arXiv:cond-mat/0207149v2 [cond-mat.str-el] 1 Oct 2002

Vacuum polarization in nanotubes

K. Sasaki[1], A. A. Farajian[2], H. Mizuseki[2], and Y. Kawazoe[2]
[1] *Department of Physics, Tohoku University, Sendai 980-8578, Japan*
[2] *Institute for Materials Research, Tohoku University, Sendai 980-8577, Japan*
(Dated: December 2, 2024)

The vacuum polarization in various types of carbon nanotubes is theoretically investigated in a model describing the π-electrons with the Coulomb interaction. It is pointed out that screened Coulomb interactions between massive fermions in metallic nanotubes weaken drastically as compared with the one in semi-conducting nanotubes. It is also shown that the Friedel oscillation around an external charge appears in un-doped armchair nanotubes depending on the value of a short length cutoff in the Coulomb interaction. A different type of oscillation is seen in metallic zigzag nanotubes which depends on the short length cutoff and a momentum cutoff of the π-electrons phase space.

I. INTRODUCTION

Vacuum structure of the π-electrons in carbon nanotubes(CNTs [1, 2, 3]) is a complicate quantum mechanical state which governs the response to an external perturbation. Many kinds of interactions [4, 5, 6, 7] are responsible for the rich vacuum structure. Among others the Coulomb interaction between electrons is the most important interaction and drives the system into a strongly correlated state [5, 6, 7]. Several aspects of the Coulomb interaction are already seen in some experiments of charging [8] and of temperature dependent resistivity [9] which are consistent with current understanding of low energy excitations in metallic CNTs. The low energy excitations in the metallic CNTs are theoretically modeled by *massless* bands (linear dispersion bands) with the Coulomb interaction as Tomonaga-Luttinger(TL) liquid [5, 6, 7]. To obtain a complete understanding of the nature of the vacuum, it is indispensable to consider a localized perturbation. As short distance physics corresponds to high energy, *massive* bands (other sub-bands except the massless bands) would come into dynamics. In this article, we focus on the effect of the π-electrons on the Coulomb interaction, namely, vacuum polarization.

It is important to study the massive bands effect because of the geometrical structure of CNTs. As an example, when we put two test charges at a distance of the order of the diameter of nanotube, the strength of one-dimensional long-range Coulomb interaction is inversely proportional to the diameter of nanotube; besides, the energy gap of the massive bands also scales as inverse of the diameter. Therefore the effect of the massive bands on the Coulomb interaction between the test particles is universal for all kinds of nanotubes. Furthermore the number of the massive bands increases as the diameter of the nanotube increases. So, for the case of CNT with large diameter or the case of multi-walled CNTs, the quantum correction to the low energy dynamics due to the massive bands would be significant. To analyze these effects, we shall construct a field theoretical model for the π-electrons and investigate the vacuum polarization. We apply the result to an analysis of the screening of an external charge in the metallic CNTs.

As for the screening, the high-energy massive mode excitations can in principle affect the screening phenomena through two different mechanisms; adding massive-fermions loop corrections to the interactions of massless bands and direct interaction of massive bands (non-perturbative effect of the massive bands on the screening phenomena). We will focus on the former mechanism. To investigate the latter, a lattice field theoretical model employing a fully self-consistent tight-binding approach including the Coulomb interaction [10, 11] would be suitable.

The paper is composed as follows. A model Hamiltonian for the π-electrons is constructed in Sec. II. In Sec. III, we quantize the π-electron fields and define propagator for each field. Then we calculate the vacuum polarization amplitude in Sec. IV and discuss the application to the screening of an external localized charge. Summary and conclusion are given in Sec. V.

II. MODEL CONSTRUCTION

We construct a continuous field theoretical model describing the π-electrons of CNTs in this section. To do this, let us begin with an electron wave function on the graphite sheet. The wave function has two components because of the honeycomb lattice structure of the graphite sheet [12],

$$\Psi_s = \begin{pmatrix} \Psi_{\bullet s} \\ \Psi_{\circ s} \end{pmatrix}, \tag{1}$$

where $s \in \{\uparrow, \downarrow\}$ is the electron spin index. A CNT can be thought of as a layer of graphite sheet folded up into a cylinder. Thus, the periodic boundary condition along the circumference of the tube forces the wave vector into discrete vectors. As a result, the electron wave function on the tube is expanded by two-components wave functions which have the discrete wave vector as,

$$\Psi_s(r) = \sum_N \psi_{Ns}(r), \tag{2}$$

where $N \in \{1, \cdots\}$ is a label for the discrete wave vector and $r = (x, y)$ are the coordinates on the surface of

the nanotube. A field theory describing the dynamics of the π-electrons in CNTs consists of the two-components fermion fields ψ_{Ns} interacting with each other via the Coulomb interaction.

Energy dispersion relation of each fermion field specifies a band structure. The band structure depends on geometry of a CNT, therefore the definition of fields also depends on it. There are two kinds of geometries: metallic and semiconducting CNTs. The metallic CNTs have linear dispersions near the Fermi points. They are contrasted with semiconducting CNTs which involve no linear dispersion near the Fermi level. The Hamiltonian density modeling these systems is given by $\mathcal{H} = \mathcal{H}_F + \mathcal{H}_C$ where $\mathcal{H}_F$ is the free (unperturbed) part and $\mathcal{H}_C$ is the perturbed part including the Coulomb interaction.

A. Kinetic term

Suppose we include only nearest neighbor tight-binding interactions, then the kinetic Hamiltonian density is given by $\mathcal{H}_F = \sum_{Ns} \mathcal{H}_N$ where

$$\begin{aligned} \mathcal{H}_N &= \psi^\dagger_{Ns} h_N \psi_{Ns} \\ &= \psi^\dagger_{Ns} V_\pi \begin{pmatrix} 0 & z(k^N_x, \hat{k}_y) \\ z^*(k^N_x, \hat{k}_y) & 0 \end{pmatrix} \psi_{Ns}. \end{aligned} \quad (3)$$

$V_\pi (= 2.7[eV])$ is the hopping integral, $\hat{k}_y = -i\partial_y$ is the wave vector along tubule axis. The discrete wave vector around the circumference is parameterized as

$$ak^N_x = -\frac{2\pi}{\sqrt{3}} + \frac{2a}{d}N, \quad (4)$$

where N is a positive integer, d is the diameter of the CNT and $a = 1.42[\mathring{A}]$ the nearest neighbor carbon-carbon spacing. Here we consider the case of metallic zigzag CNTs [13]. The function $z(k_x, k_y)$ indicates the hopping amplitude between two sub-lattices(or two components) and is defined as

$$z(k_x, k_y) = \sum_i e^{ik\cdot u_i}, \quad (5)$$

where the vector u_i is a triad of vectors pointing in the direction of the nearest neighbors of a carbon site [12]. The free Hamiltonian densities whose wave vector is equal to $ak^N_x = -\frac{4\pi}{3\sqrt{3}}$ or $\frac{4\pi}{3\sqrt{3}}$ describe massless fermions (electrons and holes in the massless bands) and the others are for massive fermions in the metallic zigzag CNTs. The low energy properties of massless fermions are analyzed successfully within the framework of TL liquid [5, 6, 7, 14].

It is straightforward to obtain a dispersion relation of the tight binding Hamiltonian using the energy eigenvalue: $\pm V_\pi |z(k^N_x, k_y)|$. We illustrate the band structure of a metallic zigzag CNT for later convenience in Fig. 1.

In the case of the zigzag CNTs, the diameter is given by the following formula

$$d = \frac{\sqrt{3}a}{\pi} N_0, \quad (6)$$

where N_0 is the number of the hexagons along the circumference. If there are nine hexagons, the diameter is $(d =) 7.04[\mathring{A}]$. The number of the bands is given by $2N_0$ which gives the correct number of the π-electrons of the system.

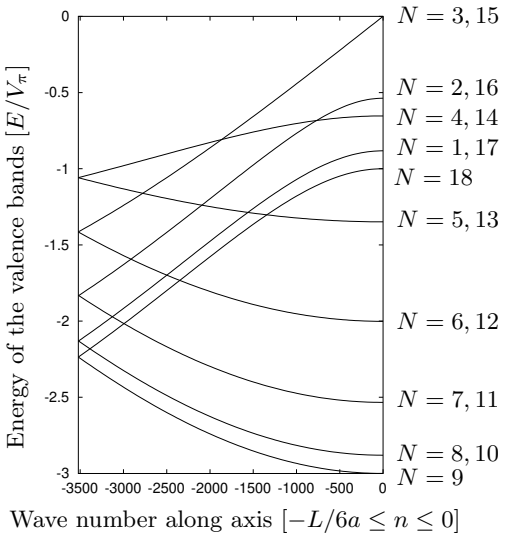

FIG. 1: Negative momentum and energy part of a band structure of the metallic zigzag CNT with $d = 7.04[\mathring{A}](N_0 = 9)$. The Fermi energy is set to zero and the horizontal axis denotes wave number. The leftmost point ($n \approx -3500$) corresponds to $k_y = 2\pi n/L = -\pi/3a$ where L is the length of the zigzag CNT and we take $L = 3[\mu\text{m}]$. Each band is labeled by N. For example, we define $N = 3(= N_0/3)$ and $N = 15(= 5N_0/3)$ to indicate two massless bands which have the same energy spectrum through K and K' Fermi points respectively.

B. Coulomb interaction

The Coulomb interaction between electrons is written using the density of the electron field Ψ_s:

$$\rho = \sum_s \Psi^\dagger_s \Psi_s = \sum_{N,s} \rho_{Ns} + \sum_{N\neq M,s} \rho_{NMs}, \quad (7)$$

where $\rho_{Ns} \equiv \psi^\dagger_{Ns}\psi_{Ns}$ and $\rho_{NMs} \equiv \psi^\dagger_{Ns}\psi_{Ms}$. ρ_{Ns} is a function of the coordinate along tubule axis, whereas ρ_{NMs} is specified by the position on the surface of CNTs. This is because there is a momentum mismatch along the circumference between ψ_N and ψ_M fields. Therefore it is possible to describe a physical quantity depending on the circumferential direction. For example, when we put an external charge on a carbon atom, the vacuum

(ground state) of the system may have an induced charge distribution around it. The induced charge density is described by the vacuum expectation value of the charge density operator:

$$\langle\rho\rangle = \sum_{N,s}\langle\rho_{Ns}\rangle + \sum_{N\neq M,s}\langle\rho_{NMs}\rangle. \quad (8)$$

The density $\langle\rho_{NMs}\rangle$ may have a non-vanishing amplitude so that it gives the circumferential dependence as $\langle\rho_{NMs}\rangle + \langle\rho_{MNs}\rangle \sim \cos(2(N-M)x/d)$. In this article we consider a circumferential *independent* perturbation and this assumption leads to $\langle\rho_{NMs}\rangle = 0$.

Using the density of the electron field, we define the Coulomb interaction as

$$H_C = \int_S \mathcal{H}_C = \frac{1}{2}\iint_S \rho(r)U(r-r')\rho(r')dr^2dr'^2, \quad (9)$$

where the integral region S denotes the surface of a nanotube and $U(r)$ is the long-range Coulomb potential,

$$U(r-r') = \frac{e^2}{4\pi}\frac{1}{\sqrt{|r-r'|^2+a_z^2}}. \quad (10)$$

$a_z = 1.33[\mathring{A}]$ is a cutoff length(thickness of the graphite sheet [6]) which corresponds to the ionization energy ($U(0) = 4V_\pi$) of a π-electron from a carbon [15] and e is the charge of electron which gives $e^2/4\pi = 1.44[\mathrm{eV}\cdot\mathrm{nm}]$. The cutoff a_z is the only parameter in the Hamiltonian which controls short distance behavior of a physical quantity, such as a charge density induced by an external charge. We do not consider a sublattice dependent interaction: $\rho_\bullet(r)\delta U(r-r')\rho_\circ(r')$, where $\rho_\bullet \equiv \sum_s \Psi^\dagger_{\bullet s}\Psi_{\bullet s}, \rho_\circ \equiv \sum_s \Psi^\dagger_{\circ s}\Psi_{\circ s}$, and $\delta U(r) \equiv \sum_i [U(r+u_i) - U(r)]$, since the potential δU is very small due to $\sum_i u_i = 0$.

Substituting Eq.(7) into Eq.(9), the Coulomb interaction is transformed into three parts:

$$H_C = H_C^a + H_C^b + H_C^c, \quad (11)$$

which are given by

$$H_C^a = \frac{1}{2}\iint_S \sum_{N,s}\rho_{Ns}(y)\ U(r-r')\sum_{N',s'}\rho_{N's'}(y')dr^2dr'^2, \quad (12)$$

$$H_C^b = \iint_S \sum_{N,s}\rho_{Ns}(y)\ U(r-r')\sum_{N'\neq M',s'}\rho_{N'M's'}(r')dr^2dr'^2, \quad (13)$$

$$H_C^c = \frac{1}{2}\iint_S \sum_{N\neq M,s}\rho_{NMs}(r)\ U(r-r')\sum_{N'\neq M',s'}\rho_{N'M's'}(r')dr^2dr'^2. \quad (14)$$

In order to get a one dimensional model, we have to integrate the circumferential degree of freedom. One can perform the integration for H_C^a, and obtain the one-dimensional long-range Coulomb interaction,

$$H_C^a = \frac{1}{2}\iint_D J(y)V(y-y')J(y')dydy', \quad (15)$$

where $V(y)$ is the unscreened Coulomb potential [6]

$$V(y) = \frac{e^2}{4\pi\sqrt{|y|^2+d^2+a_z^2}}\frac{2}{\pi}K\left(\frac{d}{\sqrt{|y|^2+d^2+a_z^2}}\right), \quad (16)$$

with $K(z)$ being the complete elliptic integral of the first kind. The internal density J is defined as the sum of individual fermion densities: $J = \sum_{Ns}\rho_{Ns}$. Here the integral region $S \in [0:\pi d]\times[0:L]$ has changed into $D \in [0:L]$ where L is the length of a nanotube.

Some comments on the one-dimensional long-range Coulomb potential are in order. It should be noted that the potential depends on the diameter of CNT. Because of that, one might think, in case of CNTs with large diameter, the Coulomb potential is weak enough to neglect the effects of the massive bands on the massless bands. But this is not the case. The band gap of the massive fermions is also scaled as $E_g \equiv V_\pi a/d$, therefore the massive bands may still affect the massless bands for CNTs with large diameter. In fact, the effect of the massive fermions on the massless fermions is universal (it does not strongly depend on the geometry). This is shown using a ratio of the potential depth and the gap energy,

$$R \equiv \frac{V(0)}{2E_g} \sim K\left(\frac{d}{\sqrt{d^2+a_z^2}}\right) > 3. \quad (17)$$

The ratio means that when two massless fermions get close to each other, more than three massive bands come into dynamics. Specifically, the massive fermions modify the Coulomb interaction between the massless fermions. We will estimate this effect using one-loop perturbation shortly. In addition, in the case of CNT with large diameter or multi-walled CNTs, the number of massive

fermions also increases so that the correction would be large.

The Fourier transform of the one-dimensional long-range Coulomb potential ($V(y) = \sum_{n\in Z}\beta_n e^{-i2\pi ny/L}$) is given by

$$\beta_n = \frac{e^2}{2\pi L}\frac{2}{\pi}\int_0^{\frac{\pi}{2}} K_0\left(\frac{2n\pi d}{L}\sqrt{\sin^2 x + \left(\frac{a_z}{d}\right)^2}\right), \quad (18)$$

where K_0 is the modified Bessel function. On the other hand, in some articles [16], the following Fourier component is used

$$v_n = \frac{e^2}{2\pi L}K_0\left(\frac{2n\pi d}{L}\right)I_0\left(\frac{2n\pi d}{L}\right). \quad (19)$$

This corresponds to the case of the potential with $\lim_{a_z\to 0} V(x)$ (or $\lim_{a_z\to 0}\beta_n$). This, in turn, would cause an infinite ionization energy of a π-electron. Because of that it is never realistic, especially for large n values. Of course, the Fourier components β_n and v_n for small n values are almost the same, and would be approximated by $\frac{e^2}{2\pi L}K_0\left(\frac{2n\pi d}{L}\right)$ [14] which corresponds to the following Coulomb potential in coordinate space,

$$V(x) = \frac{e^2}{4\pi}\frac{1}{\sqrt{|x|^2+d^2}}. \quad (20)$$

As for H_C^b, it gives no contribution when one integrates over the x and x' circumferential coordinates. However H_C^c affects the dynamics in the one dimensional system. In the case of $N - M + N' - M' = 0$, the integration can not make the H_C^c term vanish. We calculate the effective Coulomb potential for this case as(we ignore the spin index here)

$$H_C^c = \frac{1}{2}\iint_D \sum_{N\neq M}^{N'\neq M'} J_{NM}(y)V_{NM}(y-y')J_{N'M'}(y')dydy', \quad (21)$$

where $J_{NM}(y)$ is defined by the following equation $\rho_{NM}(r) = e^{-i(k^N-k^M)x}J_{NM}(y)$ and the potential is

$$V_{NM}(y) = \frac{e^2}{4\pi\sqrt{|y|^2+d^2+a_z^2}} \times \frac{1}{\pi}\int_0^{\pi}\frac{\cos 2(N-M)x}{\sqrt{1-\left(\frac{d}{\sqrt{|y|^2+d^2+a_z^2}}\right)^2\cos^2 x}}dx. \quad (22)$$

This potential is short range in case of $N \neq M$, and also weak as compared with the previous Coulomb potential (Eq. 16 corresponds to the $N = M$ case) for generic single-wall CNTs. To see this, we plot these potentials as a function of the axial coordinate for a CNT with a typical diameter in Fig. 2.

Here let us examine the effect of H_C^c term and the relationship between H_C^a and H_C^c interactions. To do so,

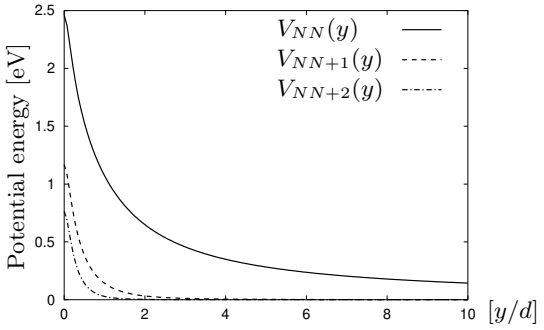

FIG. 2: Coulomb potentials for a CNT with $d = 1.4$[nm] in diameter. The solid line expresses the potential given in Eq. 16.

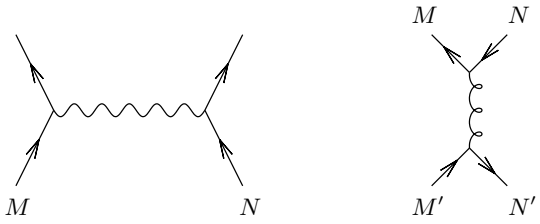

FIG. 3: Feynman diagrams for H_C^a(left) and H_C^c(right).

we draw Feynman diagrams corresponding to both interactions in Fig. 3. The left diagram stems from H_C^a interaction because J in the interaction is written by the sum of individual densities $J = \sum_N \rho_N$(here we neglect the coordinate and the spin indices) and expresses a process generated by $\rho_N V \rho_M$ term. Due to the long-range nature of the potential V, not only short-wavelength mode but also long-wavelength mode of the density couples to the Coulomb interaction. On the other hand, the potential in the right diagram is very short-range for realistic diameters(not huge) so that only short-wavelength mode of J_{NM} can feel this type of interaction.

One may regard $\sum_{N\neq M} J_{NM}(y)$ operator in H_C^c interaction as a sum of position dependent current operators $\sum_{N\neq 0} j_N(y)$ where $j_N(y) \equiv \sum_M J_{MM+N}(y)$ and of course $j_0(y) = J(y)$. When the diameter is huge, the current operator satisfies a standard current commutation relation

$$\left[j_{L(R),N}(y), j^\dagger_{L(R),N'}(y')\right] = N\delta_{NN'}\delta(y-y'), \quad (23)$$

where we assume the following decomposition: $j_N \equiv j^\dagger_{L,N} + j_{R,N}$. In terms of the current operators, $H_C^a + H_C^c$ is written as

$$H_C^a + H_C^c = \frac{1}{2}\iint_D \sum_N j_N^\dagger(y)V_N(y-y')j_N(y')dydy', \quad (24)$$

where $V_N(y) \equiv V_{MM+N}(y)$($H_C^a$ interaction corresponds to $N = 0$ term: $j_0^\dagger V_0 j_0$). The effect of the right diagram

can be estimated by the ratio between the Fourier transform of the potential $V_N(\equiv \sum_{n\in Z}\beta_n^N e^{-i2\pi ny/L})$ and the energy gap between M and $M+N$ bands $E_g \sim V_\pi a/d$ as β_n^N/E_g. Hence the effect of H_C^c is negligible for generic single-wall CNTs, however in case of huge diameter, the right diagram becomes effective. To analyze it, it is helpful to remember that the band indices are actually momentum labels. From this viewpoint, the H_C^c interaction describes the dynamics along the circumferential direction just as the H_C^a relates the dynamics along the axis. This is because H_C^a interaction is given by

$$H_C^a = \sum_n j_{0,n}^\dagger \beta_n^0 j_{0,n}, \quad j_0(y) = \sum_{n\in Z} j_{0,n} e^{-i\frac{2\pi ny}{L}} \tag{25}$$

which has the same structure as Eq.(24) replacing n(wave number along axis) with N(wave number along circumference).

Therefore, neglecting the right diagram in Fig. 3 is to ignore the dynamics along the circumferential direction. Physically speaking, a tube with huge diameter is close to the graphite sheet, thus not only the electron dynamics in axial direction but also in circumferential direction can contribute the screening of an external charge put on a carbon cite [17]. As we have commented in the beginning of this section, only circumferential independent perturbations are considered in the present paper which results in $\langle J_{NM}\rangle = 0$. This is consistent with the assumption $H_C^c = 0$. Hence, a simple model for the π-electrons in CNTs is

$$H = H_F + H_C^a, \tag{26}$$

where $H_F \equiv \int_D \mathcal{H}_F$. In this article we will use this Hamiltonian. As a result, one can not extent a theoretical result which is obtained from the above Hamiltonian to CNTs with huge diameter since, in order to analyze such tubes, we should keep the interaction H_C^c in the model.

In order to study the physics at very low energy scale, it is sufficient to investigate the low energy excitations in the system. Low energy excitations in metallic CNTs are described by a field theory of four massless fermions interacting with each other and with massive fermions through the long-range Coulomb interaction. The massive fermions modify the Coulomb potential between massless fermions because of the vacuum polarization. We will investigate this effect in the following sections.

III. QUANTIZATION OF FERMIONS

We have specified the Hamiltonian that describes the π-electron dynamics in CNTs. In this section we quantize the fermion fields and define the propagator of each field. The spin index of the electrons is suppressed in this section for simplicity.

The energy eigenfunctions of the first quantized kinetic Hamiltonian are classified into ψ_N^+ and ψ_N^- that are specified by the energy eigenvalue equations:

$$h_N \psi_N^\pm(k_n) = \pm\Delta_N(k_n)\psi_N^\pm(k_n). \tag{27}$$

ψ_N^+ is the fermion wave function which has a positive energy eigenvalue and ψ_N^- is the one whose energy eigenvalue is negative as compared with the Fermi energy. These eigen functions are given explicitly by,

$$\psi_N^\pm(k_n) = \frac{1}{\sqrt{2L}\Delta_N(k_n)} \begin{pmatrix} V_\pi z_N(k_n) \\ \pm\Delta_N(k_n) \end{pmatrix} e^{ik^\pm\cdot r}, \tag{28}$$

where the exponent is defined as $k^\pm \cdot r \equiv \mp\Delta_N(k_n)t/\hbar + k_y^n y$. Here we use the normalization condition $\int_D \psi_N^{\pm\dagger}\psi_N^\pm dy = 1$ and define the amplitude $z_N(k_n) \equiv z(k_x^N, k_y^n)$. Because of this definition, the energy eigenvalues lead to

$$\Delta_N(k_n) \equiv V_\pi |z_N(k_n)|. \tag{29}$$

The wave vector along the nanotube axis is quantized by the boundary condition. We take the periodic boundary condition for simplicity and obtain,

$$k_y^n = \frac{2\pi}{L} n \equiv k_n. \tag{30}$$

Using the above eigenfunctions, we construct the quantum fields for the π-electrons as

$$\psi_N = \sum_n \psi_N^+(k_n)a_N(k_n) + \psi_N^-(k_n)b_N^\dagger(k_n). \tag{31}$$

$a_N(k_n), b_N(k_n)$ are independent fermionic annihilation operators of positive and negative energy fermion species labeled by N whose wave vector is k_n and their anticommutation relations are

$$\{a_N(k_n), a_M^\dagger(k_m)\} = \delta_{NM}\delta_{nm}, \tag{32}$$

$$\{b_N(k_n), b_M^\dagger(k_m)\} = \delta_{NM}\delta_{nm}. \tag{33}$$

All of the other anticommutators vanish. The massive mode dynamics is difficult to solve non-perturbatively. Hence we shall use perturbation about the Coulomb charge. To do this, we define the propagator as

$$i\Delta_F^N(x;y) \equiv \langle vac|T\{\psi_N(x)\psi_N^\dagger(y)\}|vac\rangle, \tag{34}$$

where T is the time ordering and the vacuum is defined by

$$a_N(k_n)|vac\rangle = 0, \quad b_N(k_n)|vac\rangle = 0. \tag{35}$$

An alternative representation of the propagator in momentum space is

$$G_N(E,k_n) = \frac{1}{E^2 - \Delta_N(k_n)^2 + i\epsilon} \times \begin{pmatrix} E & V_\pi z_N(k_n) \\ V_\pi z_N^*(k_n) & E \end{pmatrix}, \tag{36}$$

where E is the energy and ϵ is a positive infinitesimal.

IV. VACUUM POLARIZATION

Making use of the propagator of the π-electrons, one can compute the amplitude of the vacuum polarization at one-loop level as

$$T_n = -\sum_{N,m} \int \frac{dE}{2\pi} \mathrm{Tr}\left[G_N(E,k_m)G_N(E,k_{m-n})\right], \quad (37)$$

where n is an integer and corresponds to the wave vector $k_n(=2\pi n/L)$ of the Coulomb potential(photon). m is also an integer and is an index of an internal fermion wave vector $k_m(=2\pi m/L)$. The first minus sign on the right is required by the presence of a fermion loop. The summention of m needs to be restricted within the Brillouin zone, so that it depends on the geometrical structure of CNT. In subsection IV A, we explain the Brillouin zone for a metallic zigzag CNT, as an example.

The vacuum polarization modifies the Coulomb interaction between two test charges. Fourier components of the modified Coulomb potential are given by

$$\bar{\beta}_n = \frac{\beta_n}{1 - T_n\beta_n}. \quad (38)$$

It should be noted that the amplitude T_n is always negative because of the fermion loop, so the Coulomb interaction weakens. By performing the energy integration in Eq.(37), we rewrite the one-loop fermion amplitude including the spin degrees as

$$T_n = -\frac{2}{V_\pi}\sum_{N,m}\frac{1}{|z_N(k_m)| + |z_N(k_{m-n})|} \times \left\{1 - \frac{\mathrm{Re}[z_N(k_m)z_N^*(k_{m-n})]}{|z_N(k_m)||z_N(k_{m-n})|}\right\}. \quad (39)$$

On the other hand, the vacuum polarization of the massless fermions is calculated exactly using the current algebra supposing that the massless bands are strictly linear bands as

$$T_n = -\frac{8}{\Delta}, \quad n \neq 0, \quad (40)$$

where $\Delta = \frac{3\pi V_\pi a}{L}$ is the single-particle level spacing which is defined under the simple periodic boundary condition. This loop amplitude leads to the screened Coulomb potential [14]:

$$\bar{\beta}_n = \frac{\beta_n}{1 + \frac{8\beta_n}{\Delta}} \quad (41)$$

which can be used in a calculation of the induced charge density around an external fixed charge on the surface of the metallic CNTs. The assumption of strictly linear dispersion is suitable for the metallic zigzag CNT as is shown in Fig. 1. However for the armchair case, the massless bands are not linear for some momentum region. Hence, we have to check if the vacuum polarization amplitude by the massless fermions loop, which is derived from Eq.(39), coincides with the previous estimation.

Let us start with the metallic zigzag CNTs which have two massless bands. The hopping amplitude is given by $z_{N_0/3}(k_m) = z_{5N_0/3}(k_m) = i\frac{3}{2}ak_m$ for all m in the first Brillouin zone with sufficient accuracy. Then one gets the same result as Eq.(40),

$$T_n = -\frac{2}{V_\pi}\sum_{0\le m\le n}\frac{2}{|\frac{3}{2}ak_m| + |\frac{3}{2}ak_{m-n}|} \times 2 = -\frac{8}{\Delta}. \quad (42)$$

This is a realization of 'one-loop exact' [18] (Only one-loop vacuum polarization amplitude gives an exact answer). Note that a vector connecting K and K' Fermi points is perpendicular to the nanotube axis, so that there is no Friedel oscillation along the axis in an induced charge density near an external charge density which has no circumferential dependence. However, when a point external charge such as dopant atom attaches to a nanotube, an induced charge density along circumference may show the Friedel oscillation.

We proceed to analyze armchair CNTs. A previous study on the vacuum polarization concluded that there is a logarithmic singularity in T_n at a special n causing the Friedel oscillation around a specific external charge [16]. In order to see such a singularity, the following condition have to be satisfied

$$|z_N(k_m)| = |z_N(k_{m-n})| = 0, \quad (43)$$

for some m in the Brillouin zone $-\pi/\sqrt{3} \le k_m \le \pi/\sqrt{3}$. For the massless band in the armchair CNTs, the condition $z_N(\pm k_F) = 0$ holds($k_F \equiv 2\pi/3\sqrt{3}a$), then the above condition can be satisfied for a particular n in the Brillouin zone. In detail, when the wave vector of the Fourier mode of the Coulomb potential satisfies $k_n = 2k_F$, a singularity appears. Therefore it may cause the oscillation in the Coulomb potential and in the induced charge density around an external charge. Taking into account the electrons within the phase space(Brillouin zone), we calculate the loop amplitude numerically. The results are shown in Fig. 4. Because of the π-electron phase space, the Fourier components of the Coulomb potential which can couple to the electron density are restricted within the following region

$$-\frac{2\pi}{\sqrt{3}} \le ak_n \le \frac{2\pi}{\sqrt{3}}. \quad (44)$$

Within the above region, a singularity of the loop amplitude exists [16]. Apart from the singularity, a small cusp structure(not singularity) arises. However this cusp, due to massless loop, is small and is masked by the massive fermions loop amplitude shown in Fig. 4. Note also that the result of Eq.(40) for massless fermions is applicable to the armchair CNT with sufficient accuracy up to $ak_n \le \pi/\sqrt{3}$. However, for higher momentum region, that is not valid because of the singularity. Several application of the loop amplitude to the calculation

of screened Coulomb potential and the induced charge density around an external charge are given in the later subsections.

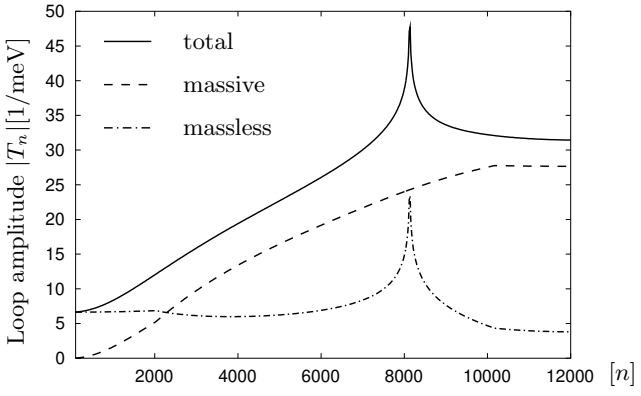

FIG. 4: Comparison between the loop amplitudes due to the massive fermions and massless fermions in an armchair CNT with $d = 6.78[\mathring{A}]$ and $L = 3[\mu m]$. At the wave vector $k_n \sim \mathcal{O}(\frac{\pi}{3\sqrt{3}})$; $(n \approx 2000)$, the effect of the massive fermions exceeds the massless fermions loop amplitude and there is a small cusp structure (not singularity). A singularity of the massless loop amplitude is shown at $k_n = 2k_F$.

In the case that the Coulomb potential is dynamic, that is, has an energy E_n, the corresponding vacuum polarization amplitude is given by

$$T_n(E_n) = -\frac{2}{V_\pi}\sum_{N,m}\frac{|z_N(k_m)|+|z_N(k_{m-n})|}{(|z_N(k_m)|+|z_N(k_{m-n})|)^2-(E_n/V_\pi)^2} \times\left\{1-\frac{\mathrm{Re}[z_N(k_m)z_N^*(k_{m-n})]}{|z_N(k_m)||z_N(k_{m-n})|}\right\}. \quad (45)$$

This formula can be used for a study of plasmon excitations, for example.

A. region of the summention

In this subsection, we explain the region of the summention of the loop momentum m in detail. To do so, we first define the phase space of the π-electrons of a metallic zigzag nanotube. Band structure of the π-electrons on the graphite sheet in the momentum coordinate is shown in Fig. 5. The first Brillouin zone is inside the solid square. The horizontal coordinates of the left edge of this square is ak_x^0 and right one is $ak_x^{2N_0}$(Eq. 4). Note that these two lines correspond to the same band. The dashed lines $N = N_0/3$ and $N = 5N_0/3$ in the square correspond to the massless bands. Because of the congruent vectors K_1 and K_2 of this space, the wave vector along the axis(y) is restricted to the following region,

$$-\frac{\pi}{3} \le ak_m \le \frac{\pi}{3}. \quad (46)$$

Let us consider a special case of $ak_n = \frac{\pi}{3}, (n = \frac{L}{6a})$ of a photon wave vector. If a massive fermion looping in a vacuum bubble diagram has also a large negative momentum $ak_m = -\frac{\pi}{3}$, then there is a fermion in the diagram with the wave vector $ak_{m-n} = -\frac{2\pi}{3}$, which is not inside the first Brillouin zone. Therefore we have to bring it back into the zone. One can do this using the congruent vectors in the space. So, such a fermion would have a different wave vector index along circumference compared to the fermion which has the wave vector $ak_m = -\frac{\pi}{3}$.

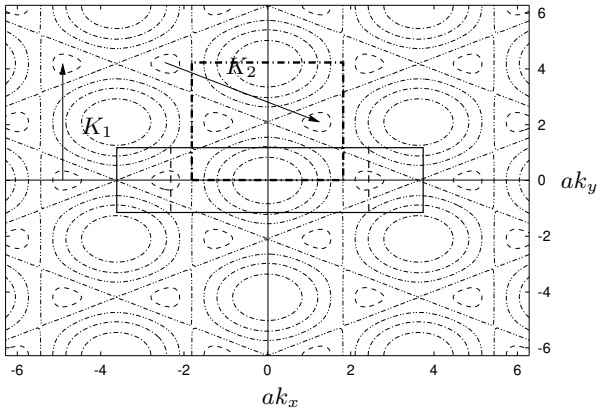

FIG. 5: Band structure of graphite sheet and the first Brillouin zone for a zigzag CNT (inside the solid square). We also depict the phase space of armchair nanotubes(inside the dot-dashed square).The vectors K_1 and K_2 are congruent vectors.

B. numerical estimation

Numerical values of both β_n and $\bar{\beta}_n$(defined below) for an armchair CNT with $d = 6.78[\mathring{A}]$ are plotted in Fig. 6. The massive fermions are observed to weaken the Coulomb interaction among the massless and massive fermions as is naturally expected. Because the Coulomb interaction between massless fermions is modified by the vacuum polarization effects of the massive fermions, the massless fermions interact with each other not via the unscreened Coulomb potential, but via the screened one whose Fourier components are given by $\bar{\beta}_n$ defined as

$$\bar{\beta}_n = \frac{\beta_n}{1-\bar{T}_n\beta_n} \quad (47)$$

where $\bar{T}_n$ is the loop amplitude due to the massive bands. We list characteristic features of $\bar{\beta}_n$.

- Long wavelength modes(small n) of the Coulomb potential between massless fermions are hardly influenced by the vacuum polarization of massive fermions. Especially, because of $T_0 = 0$, the zero mode $\bar{\beta}_0$ is equal to β_0 which means that the charging energy does not change by the inclusion of massive bands loop correction.

- The effect of massive bands loop correction cannot be taken into account by a simple introduction of

dielectric constant. The correction depends on the value of n.

Moreover, in the metallic nanotube, the massless fermions screen the Coulomb interaction between two test charges too. Hence, real Fourier component of the Coulomb interaction between them is given by

$$\tilde{\beta}_n = \frac{\beta_n}{1 - T_n \beta_n}, \tag{48}$$

which is also shown in Fig. 6. Here T_n includes all the π-electrons(massive and massless) vacuum polarization effects. The Coulomb interaction in the semiconducting CNTs is screened by the massive fermion loop only. Then, the interaction between the test charges are given by $\bar{\beta}_n$. Whereas the Coulomb interaction between massive bands in metallic CNTs has a very weak effective coupling $\tilde{\beta}_n$, but that is not so in the semiconducting CNTs because of the absence of the massless fermion's loop. Although the loop amplitude of massless fermions in armchair nanotubes has a singularity, the effect of the singularity on the screened Coulomb potential $\tilde{\beta}_n$ is small because of the smallness of β_n itself.

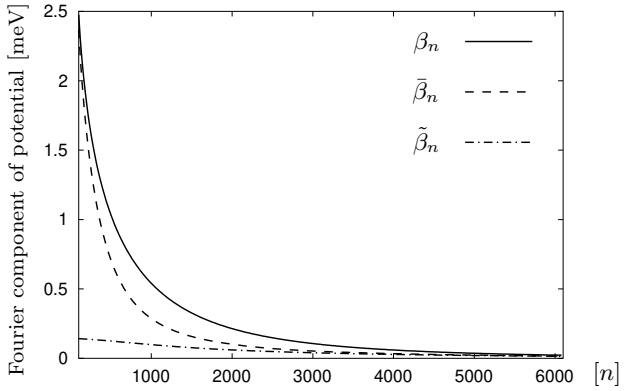

FIG. 6: Fourier component of the unscreened Coulomb potential β_n and the one modified by the vacuum polarization of the massive bands,$\bar{\beta}_n$. We also plot the modified components $\tilde{\beta}_n$ of the Coulomb interaction between two external (test) charges in metallic nanotube. Here we take the case of an armchair nanotube with $d = 6.78$ [Å] and $L = 3[\mu\text{m}]$. We set the following cutoff of the Coulomb interaction $a_z = 1.33[\mathring{A}]$.

We should examine the most effective bands in the vacuum polarization, except the massless bands contribution. Naively the lower-most energy bands except the massless bands would be the relevant bands. To check this we plot the amplitude T_n in Fig. 7 including the massive bands labeled by N for metallic zigzag CNT and compare it with an amplitude including all the massive bands. From this figure, we conclude that the low energy massive bands effectively contribute to the total amplitude(all massive bands), however, it indicates that one cannot neglect the effect of the other massive bands.

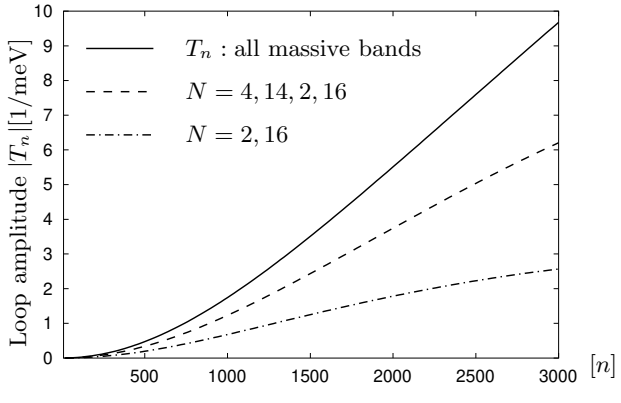

FIG. 7: Absolute value of the loop amplitude $|T_n|$ due to specific massive fermions for a metallic zigzag CNT with $d = 7.04[\mathring{A}]$ and $L = 3[\mu m]$. To understand the definition of the band index N, see Fig. 1.

C. screening

An external charge density can be included by replacing J with $J + J^{ex}$ in the Coulomb interaction (Eq. 15) where J^{ex} is a c-number whose integral over the nanotube length is equal to the total external charge. Here we take a point external charge distribution which is modeled by $J^{ex} = \delta(x - x_0)$ where x_0 is the position of the external charge along the tubule axis. The configuration of the external charge has a symmetry around the circumference of a tube.

In order to investigate the screening of the external point charge, we have to examine the ground state(vacuum) of the following Hamiltonian [19]:

$$H(J^{ex}) = H_F + \frac{1}{2}\iint_D (J + J^{ex})V(J + J^{ex}), \tag{49}$$

where the coordinate index is omitted here for simplicity. Let us define the ground state of this Hamiltonian as $|J^{ex}\rangle$. The best way to check if the screening occurs is to calculate the vacuum expectation value of the internal density: $\langle J^{ex}|J(x)|J^{ex}\rangle$. When the vacuum expectation value(VEV) is equal to a VEV without the external charge, $\langle J^{ex}|J(x)|J^{ex}\rangle = \langle 0|J(x)|0\rangle$, it means there is no-screening. The Hamiltonian including only massless bands, with an assumption of strictly linear dispersions, possesses an interesting vacuum structure, and an analytical calculation [14] of the VEV employing Tomonaga method provides an induced charge density with finite screening length. Therefore, in metallic nanotubes, there is screening. In the opposite direction, i.e., complete screening, exact cancellation of the external charge $\langle J^{ex}|J(x)|J^{ex}\rangle = -\delta(x - x_0)$ also cannot happen because of the finite strength of the Coulomb potential. Therefore a charge cloud around the external charge has finite screening length which we would like to estimate.

Up to here, we have treated the massive bands sector as perturbation [20] and calculated the effect of mas-

sive bands on the Coulomb potential between massless fermions: $\bar{\beta}_n$(Eq. 47). Assuming strictly linear dispersion of massless bands(this assumption is shown to be a valid approximation for metallic zigzag nanotubes in the beginning of the present section, and using the current algebra, one can solve the system and find the ground state in the presence of the external charge. The VEV of the density is given by the following formula [14, 21]

$$\langle J(x)\rangle = \sum_{n>0} -\frac{\frac{8\bar{\beta}_n}{\Delta}}{1+\frac{8\bar{\beta}_n}{\Delta}}\frac{2}{L}\cos\left(\frac{2\pi n}{L}(x-x_0)\right). \quad (50)$$

The assumption of strictly linear dispersion does not hold with sufficient accuracy in armchair nanotubes. So, it may be better to adopt another approach. Here we use the self-consistent-field(SCF) approximation which gives the above (exact) result supposing the strictly linear dispersion relation. In this framework, the induced charge density is defined as

$$\langle J(x)\rangle_{\rm SCF} = \sum_{n>0} \frac{\tilde{T}_n\bar{\beta}_n}{1-\tilde{T}_n\bar{\beta}_n}\frac{2}{L}\cos\left(\frac{2\pi n}{L}(x-x_0)\right). \quad (51)$$

In Figs. 8, 9 and 10, the induced charge distributions around the external point charge for both armchair and metallic zigzag CNT are depicted. It can be shown analytically that the screening length is about the diameter of the nanotube for both cases and is not sensitive to the length of the nanotube [14]. Let us remark characteristic features of the induced charge density in armchair and zigzag nanotube.

- When we apply the SCF formula to an armchair nanotube, a small oscillation appears in the case of shorter cutoff $a_z = 1.33[\mathring{A}]$ which is not shown in Fig. 8. Hence we conclude that it originates from the singularity in the massless loop amplitude. However its effect is small so that when we take an weaker cutoff $a_z = 2.66[\mathring{A}]$ we cannot see such an oscillation.

- As for the zigzag nanotube, similar oscillation appears. Because there is no singularity in the loop amplitude for zigzag nanotube, this oscillation is produced by the phase space cutoff n in the induced charge density formula Eq. 50.

In addition to the Coulomb interaction given in Eq.(15), lattice structure of the graphite may generate non-linear interactions which couple to the total charge density in armchair nanotubes [7]. Therefore it is important to examine the screening in the presence of the non-linear interactions. We discuss their effect on screening here. The induced charge density corresponds to a kink when we use the phase variable $\langle\theta(x)\rangle = 2\pi\int^x\langle J(x')\rangle dx'$, and the energy scale of the non-linear interactions is believed to be of order of the level spacing energy Δ. Hence the kink solution may increase the vacuum energy by an energy of the order of Δ, as compared with the vacuum

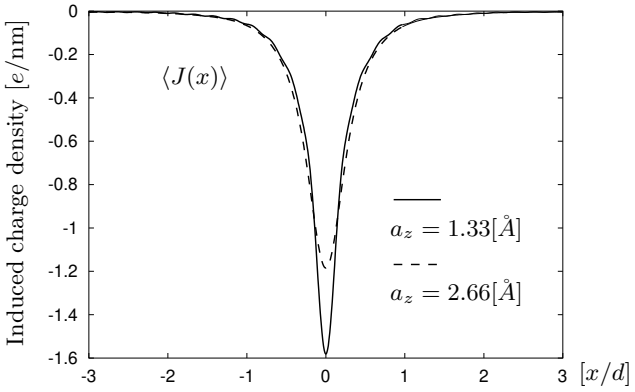

FIG. 8: Induced charge densities (including spin degeneracy) along the nanotube axis for armchair CNTs with $d = 6.78[\mathring{A}]$ and $L = 3[\mu m]$. An external unit charge locates at the origin. We plot two cases of the cutoff a_z. Theoretical curves are given by the formula Eq.(50).

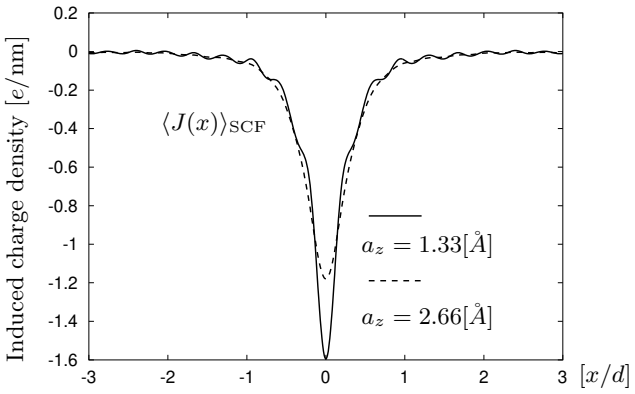

FIG. 9: Induced charge densities (including spin degeneracy) along the nanotube axis for the same armchair CNTs used in Fig.8. These curves are given by the SCF formula Eq.(51).

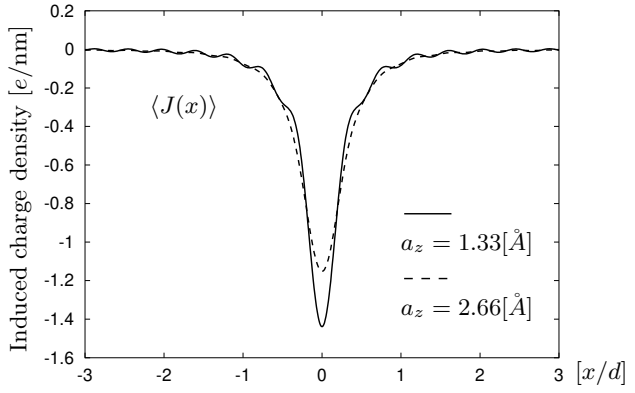

FIG. 10: Induced charge densities (including spin degeneracy) along the nanotube axis for metallic zigzag CNT with $d = 7.04[\mathring{A}]$ and $L = 3[\mu m]$. An external unit charge locates at the origin.We plot two cases of the cutoff a_z.

energy in the absence of the interactions. This small change of the vacuum energy does not affect the above conclusions.

V. SUMMARY AND DISCUSSION

In summary, we have constructed a field theoretical model of the π-electrons in metallic and semiconducting CNTs and calculated the vacuum polarization amplitude for several single-wall CNTs at one-loop level. The massive and massless bands are shown to have important role in the spectrum of the Coulomb interaction in nanotubes, through the modification of the Coulomb potential by the vacuum polarization. We also found that the finite phase space of the π-electron generates the cutoff(a_z) dependent oscillation in the induced charge density which cannot be distinguished from the Friedel oscillation.

Throughout this paper, we do not take into account two physical effects, curvature effect that make a gap in metallic zigzag nanotubes [4, 22] and boundary (cap) effect. It is easy to include the former effect in the present calculation of the loop amplitude T_n by adding an $\mathcal{O}(a/d^2)$ (fictitious) gauge field to the wave vector along the circumference k_x^N(Eq.4). If the curvature induced energy gap is small(large diameter case), this effect is negligible as we have mentioned in the end of Sec. IV. As for big energy gap, from the present perturbative calculation, we may conclude that an external charge is not screened. However non-perturbative dynamics may be still effective for the screening phenomena which needs further study on screening in nanotubes. It is also difficult to examine the latter effect, that is the π-electron dynamics near the realistic boundary with the Coulomb interactions [23].

Here, we mention the relationship between our results and a previously published article studying the effects of the massive bands. M.F. Lin and D.S. Chuu [16] are the first who were concerned with the effect of the massive bands on impurity screening at finite temperature. Their main conclusion that a metallic nanotube could screen a charged impurity with finite screening length, is shown to be valid. They show that the screening length is sensitive to the diameter of metallic nanotubes with small diameter. However, this fact would not be applicable to the nanotube with large diameter in which H_C^c interaction becomes effective.

Finally we would like to briefly discuss the vacuum polarization effect in multi-walled CNTs. The number of the massive bands increases as the diameter becomes bigger and the energy gap decreases at the same time. Therefore it is naturally expected that the vacuum polarization correction on the long wave length modes of the Coulomb interaction is large. This may cause the interesting phenomena of low energy excitations in the multi-walled CNTs. For example, the Coulomb interaction in multi-walled nanotubes consists of intra and inter layer interactions [24]. The intralayer interactions are expected to weaken by the massive bands vacuum polarization which may cause an instability of the capacitance mode [25].

[1] S. Iijima, Nature, **354**, 56 (1991).
[2] C. Dekker, Phys. Today **52**, No. 5, 22 (1999).
[3] J. W. G. Wildöer et al., Nature, **391**, 59 (1998); T. W. Odom et al., Nature, **391**, 62 (1998).
[4] C.L. Kane and E.J. Mele, Phys. Rev. Lett. **78**, 1932 (1997); P.E. Lammert and V.H. Crespi, Phys. Rev. B **61**, 7308 (2000).
[5] C. Kane, L. Balents and M.P.A. Fisher, Phys. Rev. Lett. **79**, 5086 (1997).
[6] R. Egger and A. O. Gogolin, Phys. Rev. Lett. **79**, 5082 (1997); Eur. Phys. J. B **3**, 281 (1998).
[7] H. Yoshioka and A.A. Odintsov, Phys. Rev. Lett. **82**, 374 (1999).
[8] S.J. Tans et al., Nature (London) **386**, 474 (1997); S.J. Tans et al., Nature (London) **394**, 761 (1998); H. Postma et al., J. Low. Temp. Phys. **118**, 495 (2000).
[9] M. Bockrath et al., Nature (London) **397**, 598 (1999); H.Postoma et al., Science **293**, 76 (2001).
[10] A.A. Farajian, K. Esfarjani and M. Mikami, Phys. Rev. B **65**, 165415 (2002).
[11] K. Sasaki et al., arXiv:cond-mat/0205637.
[12] The definitions of subscripts $\bullet$ and $\circ$ in Eq. 1 and the vector u_i in Eq. 5 are found in the following articles: K. Sasaki, Phys. Lett. A **296**, 237 (2002); K. Sasaki, Phys. Rev. B **65**, 155429 (2002).
[13] As for the armchair CNTs, one can use the following parameterization of the discrete wave vector:

$$ak_y^N = \frac{2a}{d}N, \quad N \in \{1, \cdots, N_0\}, \tag{52}$$

where $d = \frac{3aN_0}{2\pi}$ is the diameter and N_0 is the number of the hexagons along the circumference.
[14] K. Sasaki, Phys. Rev. B **65**, 195412 (2002).
[15] R.G. Pearson, Inorg. Chem. **27**, 734 (1988).
[16] M.F. Lin and D.S. Chuu, Phys. Rev. B **56**, 4996 (1997). The cutoff a_z(thickness of graphite sheet which stems from the extended nature of the π-electron wave function) is not taken into account in this paper. The absence of this cutoff leads to the strong Friedel oscillation because Fourier transform of the Coulomb potential has a big component at $2k_F$. The cutoff is required for the Coulomb potential between internal electrons and also between internal electrons and an external charge.
[17] D. P. DiVincenzo and E. J. Mele, Phys. Rev. B **29**, 1685 (1984).
[18] J. Schwinger, Phys. Rev. **128**, 2425 (1962).
[19] One can omit the self interaction term of an external charge,

$$\frac{1}{2}\iint_D J^{ex} V J^{ex} \tag{53}$$

from the Hamiltonian. Without this term, the energy of the system decreases after the screening of an external charge which means that the system changes into a more stable state if the external charge is screened.

[20] What we cannot take into account in the perturbation is a non-perturbative effect in screening phenomena. For example, the kinetic terms of some massive bands are approximated by the sine-Gordon model. Hence kink solutions may become effective for screening the external charge. The non-perturbative aspect of the screening can be analyzed by a lattice treatment of the nanotube system. A lattice calculation [11] of the induced charge density around the external charge shows very similar pattern to the results in the present paper.

[21] We have to specify the cutoff of n in order to calculate the vacuum expectation value of the internal density. We impose $n \leq L/\sqrt{3}a$ for armchair CNTs and $n \leq L/3a$ for zigzag CNTs. The momentum cutoff causes an oscillatory pattern [14] of the induced charge density in general. Note that this oscillation subsides when we take weaker cutoff a_z in the Coulomb potential (see Figs. 8 and 10).

[22] M. Ouyang et al., Science **292**, 27 (2001).

[23] As for the Friedel oscillation at open boundary, see the following article; H. Yoshioka and Y. Okamura, J. Phys. Soc. Jpn. **71**, No10, (2002)

[24] R. Egger, Phys. Rev. Lett. **83**, 5547 (1999).

[25] K. Sasaki, arXiv:cond-mat/0207192.